63 (2018) APPLICATIONS OF MATHEMATICS No. 6, 713–737

POLYNOMIAL CHAOS IN EVALUATING FAILURE PROBABILITY: A COMPARATIVE STUDY

Eliška Janouchová, Jan Sýkora, Anna Kučerová, Praha

Received November 27, 2017. Published online December 3, 2018.

Abstract. Recent developments in the field of stochastic mechanics and particularly regarding the stochastic finite element method allow to model uncertain behaviours for more complex engineering structures. In reliability analysis, polynomial chaos expansion is a useful tool because it helps to avoid thousands of time-consuming finite element model simulations for structures with uncertain parameters. The aim of this paper is to review and compare available techniques for both the construction of polynomial chaos and its use in computing failure probability. In particular, we compare results for the stochastic Galerkin method, stochastic collocation, and the regression method based on Latin hypercube sampling with predictions obtained by crude Monte Carlo sampling. As an illustrative engineering example, we consider a simple frame structure with uncertain parameters in loading and geometry with prescribed distributions defined by realistic histograms.

Keywords: uncertainty quantification; reliability analysis; probability of failure; safety margin; polynomial chaos expansion; regression method; stochastic collocation method; stochastic Galerkin method; Monte Carlo method

MSC 2010: 41A10, 62P30

1. Introduction

Reliability analysis and modelling of structures in general need to take into account all relevant information as well as any uncertainties in environmental conditions, loading, or structural properties. Input uncertainties influence the behaviour of the investigated system, which thus also becomes uncertain. Description of this phenomenon is provided with an uncertainty quantification process. Extensive development of efficient methods for stochastic modelling enables uncertainty quantification, even for complex models.

The research has been financially supported by the Czech Science Foundation, project No. 15-07299S.

Methods quantifying uncertainties can be classified into two groups: (i) reliability analysis methods such as the first- and second-order reliability method (FORM/SORM [8]) for computing the probability of failure related to limit states; (ii) higher moment analysis focused on estimation of higher-order statistical moments of structural response such as stochastic finite element methods (SFEM), see [23], [30], [14] for a review. SFEM is a powerful tool in computational stochastic mechanics extending the classical deterministic finite element method (FEM) to the stochastic framework involving finite elements whose properties are random [13].

In this contribution, we concentrate on SFEM based on polynomial chaos expansion (PCE) [31]. PCE is used to accelerate reliability analysis by replacing time-consuming FEM simulations within the Monte Carlo (MC) sampling of failure probability [21], [20], [27], [17]. To this end, PCE can be employed in two ways: (i) as an approximation of the model response—typically displacements (subsequently referred to as *Variant A*) or (ii) as an approximation of the resulting safety margin (*Variant B*). While statistical moments for any approximated quantity can then be computed analytically from the PCE coefficients, failure probability still needs to be estimated from MC simulations. The acceleration of the latter case comes from the replacement of an FEM simulation with rapid evaluation of the constructed PCE. The efficiency of SFEM thus depends on the computational requirements of PCE construction and its consequent accuracy.

There are several methods for constructing PCE-based surrogates: the regression method [4], [5], [7], the stochastic collocation methods [2], [32], and the stochastic Galerkin method [13], [3], [24], [9]. The principal differences between these methods are outlined. The regression method constructs the polynomial approximation of a response by using the least squares method. It is a stochastic method based on a set of model simulations performed for a stochastic design of experiments, usually obtained using Latin Hypercube Sampling. PCE coefficients are then obtained by regression of the model outputs at the design points. This leads to a solution of a system of equations. In contrast, the stochastic collocation method is a deterministic method involving a set of model simulations on a sparse grid constructed for a chosen level of accuracy. The computation of PCE coefficients is based on an explicit formula. The stochastic Galerkin method leads to a solution of a large system of deterministic equations and requires an intrusive modification of the numerical model itself [11], [29]. These methods were compared within the uncertainty quantification of stiff systems in [6]. The aim of this paper is to extend the previous work presented in [19] devoted to a comparison of these methods in the prediction of failure probability in reliability analysis. In particular, we compare the three methods in terms of computational requirements and the resulting accuracy for failure probability of a simple frame structure, where uncertain parameters occur in the geometry

of a structure and its loading [12]. The underlying random variables are described by discrete histograms to illustrate a common situation in engineering practice.

Methods for construction of PCE-based surrogates are briefly recalled in the following section. The selected example of a frame structure with uncertain parameters is described in Section 3, followed by a numerical study in Section 4. The obtained results are then summarized in Section 5.

2. Polynomial chaos expansion

In order to accelerate the sampling procedure for an uncertainty quantification process, the evaluations of a numerical model

$$\boldsymbol{r} = g(\boldsymbol{m}), \tag{2.1}$$

where $\boldsymbol{r} = (r_1, \ldots, r_{n_\mathrm{r}})^\mathrm{T}$ is a vector of model responses and $\boldsymbol{m} = (m_1, \ldots, m_{n_\mathrm{m}})^\mathrm{T}$ is a vector of random model input parameters, can be replaced by evaluations of a model surrogate. In the stochastic model problem, we assume the model parameters $\boldsymbol{m}$ to be random variables defined over some probability space $(\Omega, \mathfrak{A}, \mathbb{P})$, where Ω is the basic probability set of elementary events, $\mathfrak{A}$ a σ-algebra of subsets of Ω, and $\mathbb{P}$ a probability measure.

In particular, we search for an approximation of response $\boldsymbol{r}$ using the polynomial chaos expansion (PCE) [23], [30]. PCE can be used to approximate the response with respect to the probability distribution of random variables. For example, Hermite polynomials are associated with Gaussian distribution, Legendre polynomials with the uniform distribution, and so on.

In the case of model variables $\boldsymbol{m}$ having another distribution, new standard random variables $\boldsymbol{\xi}$ with the appropriate distribution defined by joint probability density function $w_{\boldsymbol{\xi}}$ must be introduced. Once we have expressed the model parameters $\boldsymbol{m}$ as functions of standard variables $\boldsymbol{\xi} = (\xi_1, \ldots, \xi_{n_\xi})^\mathrm{T}$, the model response also becomes a function of these variables. In this paper, we assume particular components of $\boldsymbol{m}$ as well as $\boldsymbol{\xi}$ to be independent random variables. When we use PCE-based approximation such that each model input is expressed as a polynomial with one standard variable (i.e., m_j is a univariate function of ξ_j), then the number of newly introduced standard variables n_ξ equals n_m. Let the random model output $\boldsymbol{r}$ be approximated by a PCE $\tilde{\boldsymbol{r}}$ whose polynomials are orthogonal to the probability density function of the distribution of $\boldsymbol{\xi}$. We write

$$\tilde{\boldsymbol{r}}(\boldsymbol{\xi}) = \sum_{\boldsymbol{\alpha}} \boldsymbol{\beta}_{\boldsymbol{\alpha}} \psi_{\boldsymbol{\alpha}}(\boldsymbol{\xi}), \tag{2.2}$$

where $\boldsymbol{\alpha} = (\alpha_1, \ldots, \alpha_{n_\xi})$ is a vector of n_ξ non-negative integer components that indicates the degrees of multivariate ponynomial $\psi_{\boldsymbol{\alpha}}(\xi_1, \ldots, \xi_{n_\xi}) = \psi_{\alpha_1}(\xi_1) \cdot \ldots \cdot \psi_{\alpha_{n_\xi}}(\xi_{n_\xi})$ with $\psi_{\alpha_j}(\xi_j)$ being univariate polynomials with a degree α_j. The vector $\boldsymbol{\beta}_{\boldsymbol{\alpha}}$ is a vector of PCE coefficients $\beta_{\boldsymbol{\alpha},i}$ corresponding to a particular component of system response r_i.

Expansion (2.2) is usually truncated to a limited number of terms, often related to n_ξ and n_p, the number of random variables and the maximal degree of polynomials, respectively [32]. Denoting $|\boldsymbol{\alpha}| = \sum_{j=1}^{n_\xi} \alpha_j$ and considering $|\boldsymbol{\alpha}| \leqslant n_\mathrm{p}$, the number of all terms is n_β given as

$$n_\beta = \frac{(n_\mathrm{p} + n_\xi)!}{n_\mathrm{p}!\, n_\xi!}. \tag{2.3}$$

Polynomial chaos-based surrogate modelling enables computation of statistical moments for an approximated model response $\tilde{r}_i$ analytically from the PCE coefficients [33]. In particular, the mean value can be computed as

$$\mu_{\tilde{r}_i} = \mathbb{E}[\tilde{r}_i] = \underbrace{\int \ldots \int}_{n_\xi} \sum_{|\boldsymbol{\alpha}| \leqslant n_\mathrm{p}} \beta_{\boldsymbol{\alpha},i} \psi_{\boldsymbol{\alpha}}(\boldsymbol{x}) w_{\boldsymbol{\xi}}(\boldsymbol{x})\, \mathrm{d}x_1 \ldots \mathrm{d}x_{n_\xi} = \beta_{\mathbf{0},i} \tag{2.4}$$

and the standard deviation as

$$\sigma_{\tilde{r}_i} = \sqrt{\mathbb{E}[(\tilde{r}_i - \mu_{\tilde{r}_i})^2]} = \sqrt{\sum_{0 < |\boldsymbol{\alpha}| \leqslant n_\mathrm{p}} \mathbb{E}[\psi^2_{\boldsymbol{\alpha}}(\boldsymbol{\xi})] \beta^2_{\boldsymbol{\alpha},i}}, \tag{2.5}$$

where

$$\mathbb{E}[\psi^2_{\boldsymbol{\alpha}}(\boldsymbol{\xi})] = \underbrace{\int \ldots \int}_{n_\xi} \prod_{j=1}^{n_\xi} (\psi^2_{\alpha_j}(x_j)) w_{\boldsymbol{\xi}}(\boldsymbol{x})\, \mathrm{d}x_1 \ldots \mathrm{d}x_{n_\xi}. \tag{2.6}$$

Specifically, the expected value of the product of Hermite polynomials, which are employed in this paper, is

$$\mathbb{E}[\psi^2_{\boldsymbol{\alpha}}(\boldsymbol{\xi})] = \prod_{j=1}^{n_\xi} \alpha_j!, \tag{2.7}$$

where α_j is a polynomial degree of the variable ξ_j in a polynomial $\psi_{\boldsymbol{\alpha}}$.

The efficiency of this method thus depends mainly on the computational demands of the PCE construction and its accuracy, likewise connected with the method chosen for the construction of the surrogate model [28], [25], [1].

2.1. Regression method. A very general method of computing PC coefficients in equation (2.2) is a well-known regression method [4]. The underlying assumption of this method is that the surrogate $\tilde{\boldsymbol{r}}$ is a linear combination of multivariate polynomials $\psi_{\boldsymbol{\alpha}}$, but does not have to be linear in the independent variables $\boldsymbol{\xi}$. The application is based on the following three steps:

(i) Preparation of data $\mathbf{X} \in \mathbb{R}^{n_\xi \times n_\mathrm{d}}$ obtained as n_d samples $\{\boldsymbol{x}_k,\, k = 1, \ldots, n_\mathrm{d}\}$ of the parameter vector $\boldsymbol{\xi}$,

(ii) Evaluation of the model for samples $\{\boldsymbol{x}_k,\, k = 1, \ldots, n_\mathrm{d}\}$ resulting in response samples $\{\boldsymbol{r}_k,\, k = 1, \ldots, n_\mathrm{d}\}$ organised into a matrix $\mathbf{R} \in \mathbb{R}^{n_\mathrm{r} \times n_\mathrm{d}}$, where n_r is the number of response components, and

(iii) Computation of PCE coefficients $\boldsymbol{\beta}_{\boldsymbol{\alpha}}$ organised into a matrix $\mathbf{B} \in \mathbb{R}^{n_\mathrm{r} \times n_\beta}$ using e.g. the ordinary least square method.

Since the most time-consuming part of this method consists in evaluating the model for samples of random variables, the choice of these samples represents a crucial task with the highest impact on computational time requirements. The simplest way is to choose samples using the Monte Carlo method, i.e., to draw them randomly from a prescribed probability distribution. However, the accuracy of the resulting surrogate depends on the quality with which the samples cover the defined domain [16]. The same quality can be achieved with a smaller number of samples when drawn according to a stratified procedure called the design of experiments (DoE). Latin hypercube sampling (LHS) is a well-known DoE able to respect the prescribed probability distributions. There also exist more enhanced ways of optimising LHS (see e.g. [18]), but these are out of scope for this paper. Here, the simplest version of unoptimised LHS is employed. Each computation of a response sample $\boldsymbol{r}_k$ then includes an evaluation of the transformations between model variables $\boldsymbol{m}$ and standard variables $\boldsymbol{\xi}$ and the evaluation of model (2.1).

The computation of PCE coefficients $\mathbf{B}$ starts with an evaluation of all polynomial terms $\boldsymbol{\psi}$ for all samples $\{\boldsymbol{x}_k,\, k = 1, \ldots, n_\mathrm{d}\}$ and saving them in a matrix $\mathbf{Z} \in \mathbb{R}^{n_\mathrm{d} \times n_\beta}$. The ordinary least square method then leads to

$$\mathbf{Z}^\mathrm{T}\mathbf{Z}\mathbf{B}^\mathrm{T} = \mathbf{Z}^\mathrm{T}\mathbf{R}^\mathrm{T}, \tag{2.8}$$

which is n_r linear systems of n_β equations.

2.2. Stochastic collocation. The stochastic collocation method [34], [26], [22], [10] is based on an explicit expression of the PCE coefficients of orthogonal polynomials with respect to the probability distribution:

$$\beta_{\boldsymbol{\alpha},i} = \frac{1}{\mathbb{E}[\psi^2_{\boldsymbol{\alpha}}(\boldsymbol{\xi})]} \underbrace{\int \ldots \int}_{n_\xi} r_i(\boldsymbol{x}) \psi_{\boldsymbol{\alpha}}(\boldsymbol{x}) w_{\boldsymbol{\xi}}(\boldsymbol{x})\, \mathrm{d}x_1 \ldots\, \mathrm{d}x_{n_\xi}, \tag{2.9}$$

which can be calculated numerically using an appropriate integration rule (quadrature) on $\mathbb{R}^{n_\xi}$. Equation (2.9) then becomes

$$\beta_{\boldsymbol{\alpha},i} \approx \frac{1}{\mathbb{E}[\psi^2_{\boldsymbol{\alpha}}(\boldsymbol{\xi})]} \sum_{l=1}^{n_\mathrm{d}} r_i(\boldsymbol{x}_l)\psi_{\boldsymbol{\alpha}}(\boldsymbol{x}_l)v_l, \tag{2.10}$$

where $\boldsymbol{x}_l$ stands for an integration node and v_l is the corresponding weight. Here we employ versions of the Smolyak quadrature rule, in particular quadratures with Gaussian rules (GQN) and nested Kronrod-Patterson quadrature rules (KPN) derived for normal distribution, see [15].

It is clear that the stochastic collocation method is similar to the regression method, because in both cases the evaluation of a set of model simulations requires the most computational effort. The principal difference can be seen in sample generation, where the stochastic collocation method uses preoptimized sparse grids while the regression method is based on stochastic LHS.

2.3. Stochastic Galerkin. The stochastic Galerkin method is principally different from the previous ones based on a set of independent model simulations. This method spreads the classical finite element method into the stochastic space given by the equation

$$\mathbf{K}(\boldsymbol{m})\boldsymbol{r} = \boldsymbol{f}(\boldsymbol{m}), \tag{2.11}$$

where $\mathbf{K}$ is an $n_\mathrm{r} \times n_\mathrm{r}$ stiffness matrix, $\boldsymbol{f}$ is an $n_\mathrm{r} \times 1$ loading vector, and $\boldsymbol{r}$ is an $n_\mathrm{r} \times 1$ unknown displacement vector. The stochastic Galerkin method is an intrusive method, i.e., it requires reformulation of this governing equation. To this end, we rewrite equation (2.2) using a matrix notation

$$\tilde{\boldsymbol{r}}(\boldsymbol{\xi}) = (\mathbf{I} \otimes \boldsymbol{\psi}^\mathrm{T}(\boldsymbol{\xi}))\boldsymbol{\beta}, \tag{2.12}$$

where $\mathbf{I} \in \mathbb{R}^{n_\mathrm{r} \times n_\mathrm{r}}$ is the identity matrix, $\otimes$ is the Kronecker product, $\boldsymbol{\psi}(\boldsymbol{\xi})$ is an n_β-dimensional column vector of polynomials, and $\boldsymbol{\beta}$ is an $(n_\beta \cdot n_\mathrm{r})$-dimensional column vector of PCE coefficients organized here as $\boldsymbol{\beta} = (\boldsymbol{\beta}_1^\mathrm{T}, \ldots, \boldsymbol{\beta}_i^\mathrm{T}, \ldots, \boldsymbol{\beta}_{n_r}^\mathrm{T})^\mathrm{T}$, where $\boldsymbol{\beta}_i = (\ldots, \beta_{\boldsymbol{\alpha},i}, \ldots)^\mathrm{T}$ consists of PCE coefficients corresponding to the ith response component.

Substituting the model response $\boldsymbol{r}$ in equation (2.11) with its PCE approximation $\tilde{\boldsymbol{r}}$ given in equation (2.12) and applying the Galerkin projection, we obtain

$$\underbrace{\int \ldots \int}_{n_\xi} \boldsymbol{\psi}(\boldsymbol{x}) \otimes \mathbf{K}(\boldsymbol{x}) \otimes \boldsymbol{\psi}^\mathrm{T}(\boldsymbol{x}) w_{\boldsymbol{\xi}}(\boldsymbol{x})\,\mathrm{d}\boldsymbol{x}\boldsymbol{\beta} = \underbrace{\int \ldots \int}_{n_\xi} \boldsymbol{\psi}(\boldsymbol{x}) \otimes \boldsymbol{f}(\boldsymbol{x}) w_{\boldsymbol{\xi}}(\boldsymbol{x})\,\mathrm{d}\boldsymbol{x}, \tag{2.13}$$

which is a linear system of $(n_\beta \cdot n_\mathrm{r})$ equations with unknowns in the vector $\boldsymbol{\beta}$. Integration can be performed numerically or analytically. The analytical solution is available e.g. when all terms in the stiffness matrix and in the loading vector are polynomials with respect to $\boldsymbol{\xi}$. In such cases, the method is called *fully intrusive*. In other cases, a numerical integration leading to a *semi-intrusive* Galerkin method is inevitable and can be again solved with help of the Smolyak integration rule, namely GQN [15].

3. Description of a frame structure with uncertain parameters

The goal of the work presented here is to compare the methods described for approximating the model response and accelerating the Monte Carlo (MC) sampling performed in order to estimate the probability distribution of the safety margin and the probability of structural failure.

In order to demonstrate the performance of the methods described on an engineering structure, we have chosen a simple frame with two beams (cross-section HEB 100) and a column (cross-section HEB 120) presented in [12]. To keep the comparison study clear, the geometry, loading conditions, input material parameters, random variables, and their corresponding notation are preserved as in [12]. As an illustration, the initial geometry and loading conditions are displayed in Figure 1.

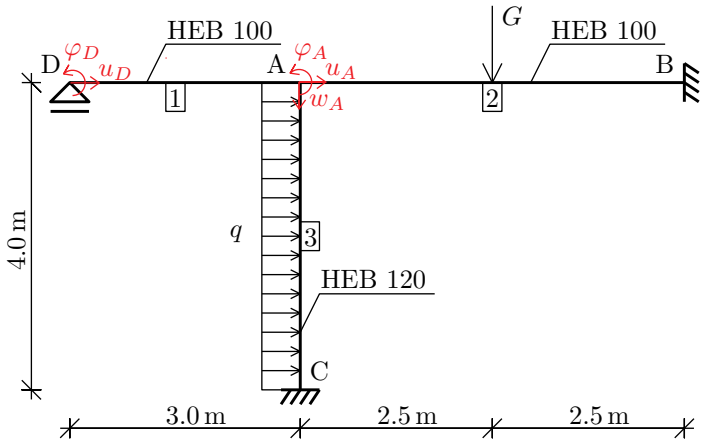

Figure 1. Scheme of the frame structure.

The frame is made of steel with Young's modulus $E = 210\,[\mathrm{GPa}]$ and uncertain yield stress f_y obtained by the product of the nominal value $f_{y,\mu}$ and the dimensionless variation $f_{y,\sigma}$ defined by a prescribed histogram (see Figure 2).

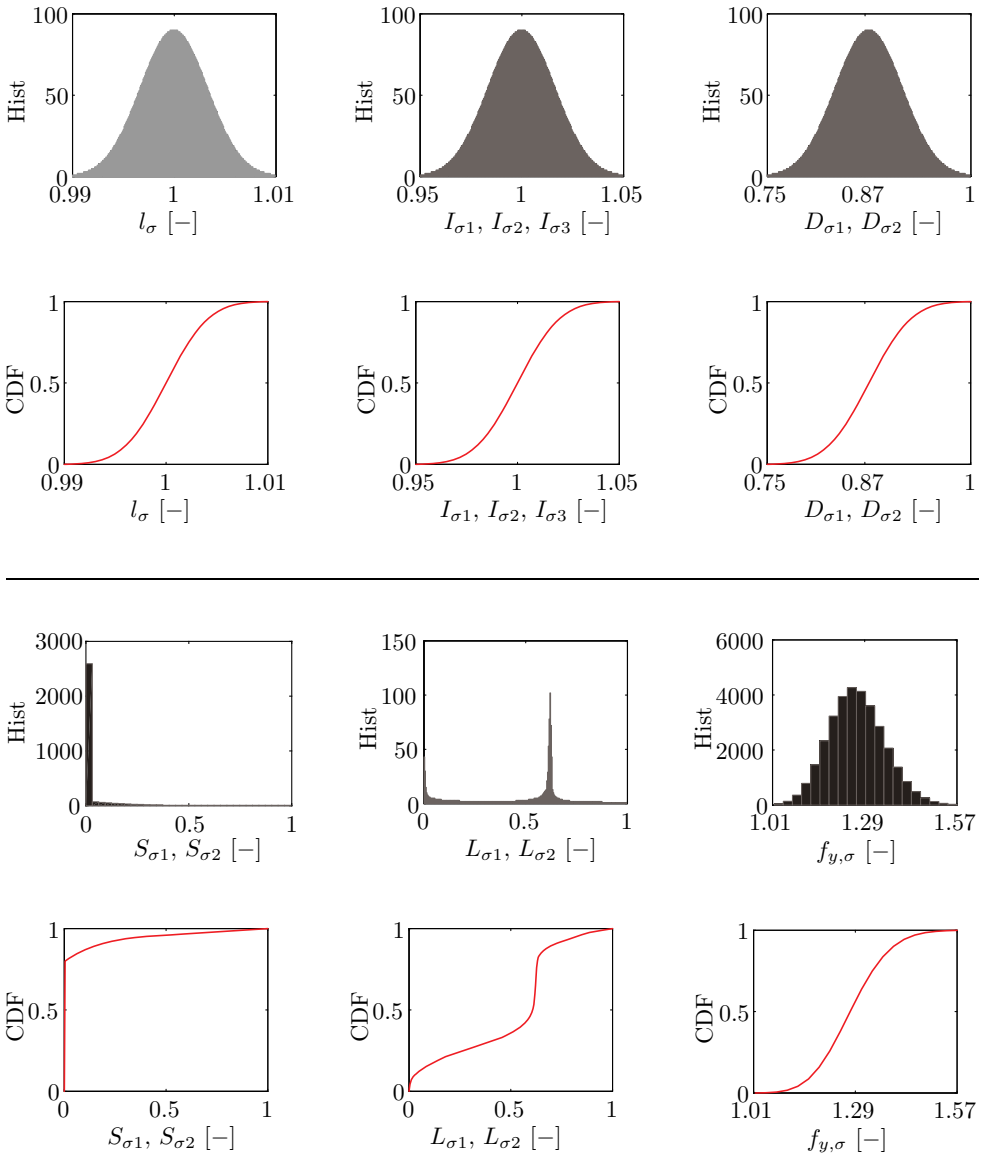

Figure 2. Histograms of uncertain parameters and the corresponding cumulative density functions.

The geometrical parameters of the particular beams are considered to be uncertain and defined as products of the corresponding nominal values and dimensionless variations given in [12] and listed in Table 1. The particular histograms are also depicted in Figure 2.

Variable	Nominal value	Dimensionless variation
Yield stress	$f_{y,\mu} = 235\,[\mathrm{GPa}]$	$f_{y,\sigma}\,[-]$
Moment of inertia	$I_1 = 449.5\ [\mathrm{cm}^4]$	$I_{\sigma 1}\,[-]$
Cross-sectional area	$A_1 = 26.04\ [\mathrm{cm}^2]$	$I_{\sigma 1}\,[-]$
Moment of inertia	$I_2 = 449.5\ [\mathrm{cm}^4]$	$I_{\sigma 2}\,[-]$
Cross-sectional area	$A_2 = 26.04\ [\mathrm{cm}^2]$	$I_{\sigma 2}\,[-]$
Moment of inertia	$I_3 = 864.4\ [\mathrm{cm}^4]$	$I_{\sigma 3}\,[-]$
Cross-sectional area	$A_3 = 34.01\ [\mathrm{cm}^2]$	$I_{\sigma 3}\,[-]$
Elastic section modulus	$W_3 = 144.1\ [\mathrm{cm}^3]$	$I_{\sigma 3}\,[-]$
Length	$l_1 = 3.0\,[\mathrm{m}]$	$l_\sigma\,[-]$
Length	$l_2 = 5.0\,[\mathrm{m}]$	$l_\sigma\,[-]$
Length	$l_3 = 4.0\,[\mathrm{m}]$	$l_\sigma\,[-]$
Dead load	$D_1 = 11\ [\mathrm{kNm}^{-1}]$	$D_{\sigma 1}\,[-]$
Short-lasting load	$S_1 = 9\ [\mathrm{kNm}^{-1}]$	$S_{\sigma 1}\,[-]$
Long-lasting load	$L_1 = 5.5\ [\mathrm{kNm}^{-1}]$	$L_{\sigma 1}\,[-]$
Dead load	$D_2 = 3.5\ [\mathrm{kN}]$	$D_{\sigma 2}\,[-]$
Short-lasting load	$S_2 = 2.2\ [\mathrm{kN}]$	$S_{\sigma 2}\,[-]$
Long-lasting load	$L_2 = 1.7\ [\mathrm{kN}]$	$L_{\sigma 2}\,[-]$

Table 1. Material, geometrical, and loading data with the corresponding variations.

The prescribed loading conditions are linear combinations of dead, long-lasting, and short-lasting load given as:

$$q = D_1 D_{\sigma 1} + S_1 S_{\sigma 1} + L_1 L_{\sigma 1}\ [\mathrm{kNm}^{-1}], \tag{3.1}$$

and

$$G = D_2 D_{\sigma 2} + S_2 S_{\sigma 2} + L_2 L_{\sigma 2}\ [\mathrm{kN}], \tag{3.2}$$

where the particular loads are statistically independent and described by random variables with nominal values $(D_1, S_1, L_1, D_2, S_2, L_2)$ and variations $(D_{\sigma 1}, S_{\sigma 1}, L_{\sigma 1}, D_{\sigma 2},\ S_{\sigma 2}, L_{\sigma 2})$ defined in Table 1 and by the histograms depicted in Figure 2.

Let us simplify the notation and denote all random variables as m_i,

$$\boldsymbol{m} = (m_1, \ldots, m_{n_m})^{\mathrm{T}} = (I_{\sigma 1}, I_{\sigma 2}, I_{\sigma 3}, l_\sigma, D_{\sigma 1}, S_{\sigma 1}, L_{\sigma 1}, D_{\sigma 2}, S_{\sigma 2}, L_{\sigma 2})^{\mathrm{T}}. \tag{3.3}$$

None of these variables has a continuous probability density function (PDF), which is necessary for constructing the PCE-based approximation, but their distribution is described by discrete histograms. For this reason, we introduce new standard random

variables $\boldsymbol{\xi} = (\xi_1, \ldots, \xi_{n_\xi})^{\mathrm{T}}$, $n_\xi = n_m$, with a continuous PDF. The variables m_j can be then expressed by transformation functions t_j with variables ξ_j, i.e.

$$m_j = t_j(\xi_j). \tag{3.4}$$

For discrete histograms, the transformation functions are non-smooth. Particular examples of transformation functions will be discussed in Section 4.

Since the axial force in the column does not achieve critical intensity, instability does not play any role and thus the column has only one failure mode determined by the material yield stress. The maximal internal forces will appear in the column at support 'C' and can be computed from the displacement and rotation of joint 'A'. The unknown displacements $\boldsymbol{r} = (u_{\mathrm{D}}, \varphi_{\mathrm{D}}, u_{\mathrm{A}}, w_{\mathrm{A}}, \varphi_{\mathrm{A}})$ can be—for the geometrical and material linearity considered here—computed using the finite element method or the displacement method, both of which are very well-known. Hence, we start directly with the latter method with a discretized form of the equilibrium equations given in equation (2.11), which—after applying the boundary conditions—comprises a system of five linear equations for the unknown vector $\boldsymbol{r} = (u_{\mathrm{D}}, \varphi_{\mathrm{D}}, u_{\mathrm{A}}, w_{\mathrm{A}}, \varphi_{\mathrm{A}})$. The stiffness matrix is given as

$$\mathbf{K} = \frac{12E}{l_\sigma} \cdot \begin{bmatrix} \frac{A_1 I_{\sigma 1}}{12 l_1} & 0 & -\frac{A_1 I_{\sigma 1}}{12 l_1} & 0 & 0 \\ 0 & \frac{I_1 I_{\sigma 1}}{3 l_1} & 0 & \frac{I_1 I_{\sigma 1}}{2 l_1^2 l_\sigma} & \frac{I_1 I_{\sigma 1}}{6 l_1} \\ -\frac{A_1 I_{\sigma 1}}{12 l_1} & 0 & k_{33} & 0 & \frac{I_3 I_{\sigma 3}}{2 l_3^2 l_\sigma} \\ 0 & \frac{I_1 I_{\sigma 1}}{2 l_1^2 l_\sigma} & 0 & k_{44} & \frac{I_1 I_{\sigma 1}}{2 l_1^2 l_\sigma} - \frac{I_2 I_{\sigma 2}}{2 l_2^2 l_\sigma} \\ 0 & \frac{I_1 I_{\sigma 1}}{6 l_1} & \frac{I_3 I_{\sigma 3}}{2 l_3^2 l_\sigma} & \frac{I_1 I_{\sigma 1}}{2 l_1^2 l_\sigma} - \frac{I_2 I_{\sigma 2}}{2 l_2^2 l_\sigma} & k_{55} \end{bmatrix}, \tag{3.5}$$

where

$$k_{33} = \frac{A_1 I_{\sigma 1}}{12 l_1} + \frac{A_2 I_{\sigma 2}}{12 l_2} + \frac{I_3 I_{\sigma 3}}{l_3^3 l_\sigma^2}, \quad k_{44} = \frac{I_1 I_{\sigma 1}}{l_1^3 l_\sigma^2} + \frac{I_2 I_{\sigma 2}}{l_2^3 l_\sigma^2} + \frac{A_3 I_{\sigma 3}}{12 l_3},$$
$$k_{55} = \frac{I_1 I_{\sigma 1}}{3 l_1} + \frac{I_2 I_{\sigma 2}}{3 l_2} + \frac{I_3 I_{\sigma 3}}{3 l_3},$$

and the loading vector as

$$\boldsymbol{f} = \begin{pmatrix} 0 \\ 0 \\ \frac{1}{2}(D_1 D_{\sigma 1} + S_1 S_{\sigma 1} + L_1 L_{\sigma 1}) l_3 l_\sigma \\ \frac{1}{2}(D_2 D_{\sigma 2} + S_2 S_{\sigma 2} + L_2 L_{\sigma 2}) \\ -\frac{(D_2 D_{\sigma 2} + S_2 S_{\sigma 2} + L_2 L_{\sigma 2}) l_2 l_\sigma}{8} + \frac{(D_1 D_{\sigma 1} + S_1 S_{\sigma 1} + L_1 L_{\sigma 1})(l_3 l_\sigma)^3}{12} \end{pmatrix}. \tag{3.6}$$

Safety margin M of the column is the difference between the yield stress f_y and the stress σ produced by the external load and given as

$$\sigma = -w_{\mathrm{A}}E + \Big(\frac{ql_3^2l_\sigma^2}{12I_{\sigma 3}} + \frac{2EI_3}{l_3l_\sigma}\varphi_{\mathrm{A}} + \frac{6EI_3}{l_3l_\sigma}u_{\mathrm{A}}\Big)\Big/W_3. \tag{3.7}$$

Failure F occurs when σ exceeds f_y. The probability of failure $\Pr(F)$ is then estimated to be the number of failures divided by the total number of performed simulations n:

$$\Pr(F) = \frac{1}{n}\sum_{s=1}^{n} I[f_y - \sigma_s \leqslant 0], \tag{3.8}$$

where $I[f_y - \sigma \leqslant 0]$ is an indicator function with value one if $f_y - \sigma \leqslant 0$, and zero otherwise.

In this numerical study, two variants of the model response are considered. For the first variant, the safety margin is calculated from the vector $\tilde{\boldsymbol{r}}$ that approximates the displacements $\boldsymbol{r}$ (*Variant A*). In the second case, the approximated random output is directly the safety margin M (*Variant B*). In the first variant, the stochastic Galerkin method can be applied and compared with the other two methods described in Section 2.

The results for the constructed surrogate models are compared with reference results obtained by MC sampling with $n = 10^7$ samples. For *Variant A*, the relative errors [%] in an estimation of the mean of the particular response components are defined as

$$\varepsilon_{\mu_i} = \frac{|\mu_{i,\mathrm{PCE}} - \mu_{i,\mathrm{MC}}|}{\mu_{i,\mathrm{MC}}} \cdot 100, \quad i = 1, \ldots, n_{\mathrm{r}}, \tag{3.9}$$

where $\mu_{i,\mathrm{MC}}$ is the MC-based estimation of the mean and $\mu_{i,\mathrm{PCE}}$ is the mean computed for a particular surrogate model. An analogous expression is also used to evaluate errors in estimating the standard deviation.

In both variants of model response, the relative errors [%] in predicting the safety margin are obtained with

$$\varepsilon_M = \frac{1}{n}\sum_{s=1}^{n} \frac{|M_{\mathrm{PCE},s} - M_{\mathrm{MC},s}|}{\max M_{\mathrm{MC}} - \min M_{\mathrm{MC}}} \cdot 100, \tag{3.10}$$

where M_{MC} stands for the samples of the safety margin estimated using the MC method. In (3.10), $M_{\mathrm{MC},s}$ and $M_{\mathrm{PCE,s}}$ stand for a particular sample of the safety margin obtained by the MC method with the full numerical model or a chosen surrogate model, respectively.

4. Numerical study

We assume that the components of $\boldsymbol{\xi}$ are standard Gaussian variables and thus we employ Hermite polynomials for the model surrogate. The study involves several variants of distributions for model parameters $\boldsymbol{m}$.

First, each model parameter m_j is distributed according to the prescribed histogram and the corresponding transformation to the standard variable ξ_j consists of two steps. The variable ξ_j is transformed using the cumulative distribution function of the standard normal distribution

$$\Phi(\xi_j) = \int_{-\infty}^{\xi_j} \frac{1}{\sqrt{2\pi}} \mathrm{e}^{-t^2/2} \,\mathrm{d}t \tag{4.1}$$

to the uniformly distributed variables on the interval $\langle 0; 1\rangle$. Then, the final transformation step is based on piecewise linear inverse cumulative distribution functions arising from the prescribed histogram.

For transformation functions, the stochastic Galerkin method can be applied in its semi-intrusive form. In our particular example, we multiply the governing equation (2.11) involving the expressions in equations (3.5) and (3.6) by $(l_\sigma)^3$ so as to obtain polynomials in terms of model parameters $\boldsymbol{m}$. However, we will not obtain polynomials in terms of $\boldsymbol{\xi}$ due to non-smooth transformations (equation (3.4)) produced by the discrete nature of the histograms prescribed to $\boldsymbol{m}$.

Table 2 contains results of uncertainty quantification for response components in terms of their means and standard deviations. These results are obtained for *Variant A*, where one PCE is used to approximate each response component. The presented methods are compared here in this specific form: the regression method (LHS), the stochastic collocation method in two variants (KPN, GQN), and semi-intrusive Galerkin method based on GQN quadrature rules (GM GQN) for four polynomial degrees n_p.

The results show good predictions obtained using the regression method, while stochastic collocation based on KPN rules leads to significant errors in estimating standard deviations, with the method based on GQN rules appearing to be even divergent. The semi-intrusive Galerkin method achieves better results in estimating standard deviations than the stochastic collocation based on the same quadrature rules. Estimated PDFs for displacement u_A depicted in Figure 3 are not sufficient, even for the regression method.

Moreover, the PCE-based approximations are compared to the polynomial approximation (PA) without orthogonality of the polynomial basis with respect to the input distribution. In this case, the polynomials approximate directly the relations between the model parameters $\boldsymbol{m}$ and the model responses $\boldsymbol{r}$. The PA coefficients are

Method	n_p	n_d	Time [s]	μ_{u_A} [mm]	σ_{u_A} [mm]	μ_{w_A} [mm]	σ_{w_A} [mm]	μ_{φ_A} [mrad]	$\sigma_{\varphi_\mathrm{A}}$ [mrad]
MC	–	10^7	22191	0.207	0.033	0.009	0.002	4.090	0.795
				$\varepsilon_{\mu_{u_\mathrm{A}}}$ [%]	$\varepsilon_{\sigma_{u_\mathrm{A}}}$ [%]	$\varepsilon_{\mu_{w_\mathrm{A}}}$ [%]	$\varepsilon_{\sigma_{w_\mathrm{A}}}$ [%]	$\varepsilon_{\mu_{\varphi_\mathrm{A}}}$ [%]	$\varepsilon_{\sigma_{\varphi_\mathrm{A}}}$ [%]
LHS	1	21	0	0.18	11.96	0.32	60.63	0.20	14.20
	2	201	0	0.26	4.76	0.36	2.49	0.34	4.41
	3	1201	3	0.08	1.36	0.01	0.02	0.10	1.54
	4	5301	19	0.02	1.31	0.09	0.98	0.04	1.21
KPN	1	21	0	4.81	9.34	4.26	8.42	4.90	9.38
	2	201	0	4.81	5.54	4.26	4.32	4.90	5.53
	3	1201	3	2.26	7.37	1.98	3.73	2.31	5.18
	4	5301	13	0.30	11.36	0.29	6.20	0.30	7.96
GQN	1	21	0	6.68	22.99	6.06	15.52	6.78	23.00
	2	221	0	4.81	73.94	4.25	50.93	4.90	58.21
	3	1581	4	3.11	59.73	2.81	37.07	3.16	46.92
	4	8761	21	1.13	187.92	1.10	129.41	1.14	147.83
GM GQN	1	21	1	0.37	17.50	1.28	16.47	0.29	19.82
	2	221	0	0.37	1.81	1.28	6.67	0.29	7.90
	3	1581	3	0.37	1.24	1.28	4.97	0.29	4.13
	4	8761	41	0.37	6.51	1.28	5.44	0.29	1.29
PA	1	21	302	0.01	0.41	0.17	1.32	$3\cdot10^{-3}$	0.36
	2	201	377	$3\cdot10^{-4}$	0.01	$1\cdot10^{-4}$	$5\cdot10^{-3}$	$2\cdot10^{-4}$	$2\cdot10^{-3}$
	3	1201	540	$5\cdot10^{-6}$	$2\cdot10^{-4}$	$2\cdot10^{-5}$	$2\cdot10^{-4}$	$1\cdot10^{-6}$	$3\cdot10^{-5}$
	4	5301	1117	$4\cdot10^{-6}$	$9\cdot10^{-5}$	$1\cdot10^{-6}$	$7\cdot10^{-5}$	$2\cdot10^{-6}$	$1\cdot10^{-5}$

Table 2. Time requirements and errors in predicting means and standard deviations of displacement vector components for the *prescribed histograms* with model parameters $\boldsymbol{m}$.

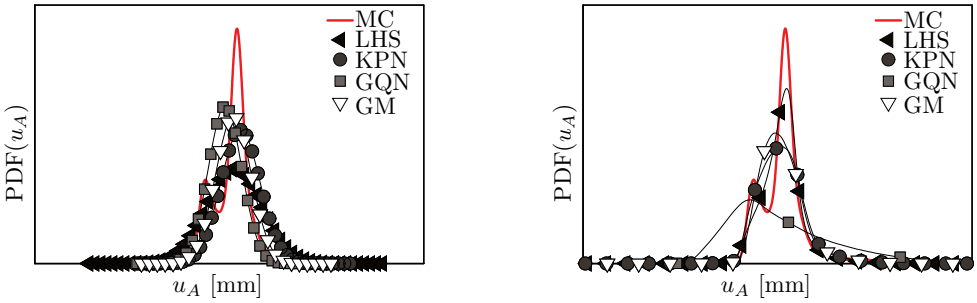

Figure 3. Probability density functions of displacement u_A for different n_p for the *prescribed histograms* with model parameters $\boldsymbol{m}$.

computed by the regression method based on LHS design respecting the prescribed histograms of the model parameters. The benefit of this approach is the elimination of the nonlinear transformation functions from the approximated relations which enables to reach a higher accuracy with the same polynomial degree in comparison with PCE, see Table 2. On the other hand, there are disadvantages associated with the computational aspects. No restrictions on the model parameters' distribution can lead to an ill-conditioned system of equations in the least square method as it occurs in this investigated case. On top of that, the polynomial coefficients cannot be used to compute statistical moments of the approximated model response analytically, but for this purpose the Monte Carlo samples of PA have to be employed, which increases the computation time.

Predictions of safety margin M and failure probability $\Pr(F)$ are summarised in Table 3 for *Variant A* as well as for *Variant B*, where PCE is used as a direct surro-

		Variant B				*Variant A*			
Method	n_p	n_d	Time [s]	$\Pr(F)$ [−]	ε_M [%]	n_d	Time [s]	$\Pr(F)$ [−]	ε_M [%]
MC	–	10^7	23825	$7\cdot10^{-5}$	–	10^7	22191	$7\cdot10^{-5}$	–
LHS	1	23	32	$7\cdot10^{-7}$	4.20	21	473	$3\cdot10^{-5}$	1.33
	2	243	164	$16\cdot10^{-5}$	2.66	201	549	$6\cdot10^{-5}$	0.63
	3	1607	757	$157\cdot10^{-5}$	2.12	1201	772	$18\cdot10^{-5}$	0.44
	4	7767	2702	$138\cdot10^{-5}$	1.79	5281	1416	$18\cdot10^{-5}$	0.37
KPN	1	23	31	$1\cdot10^{-6}$	4.31	21	487	$2\cdot10^{-5}$	0.88
	2	243	164	$49\cdot10^{-5}$	3.11	201	547	$9\cdot10^{-5}$	0.64
	3	1607	760	$113\cdot10^{-5}$	2.98	1201	801	$13\cdot10^{-5}$	0.59
	4	7767	2701	$84\cdot10^{-5}$	3.43	5281	1416	$11\cdot10^{-5}$	0.65
GQN	1	23	31	0	3.51	21	475	$4\cdot10^{-6}$	0.71
	2	265	164	$5\cdot10^{-5}$	9.75	221	549	$4\cdot10^{-5}$	1.78
	3	2069	764	$719\cdot10^{-5}$	6.98	1581	759	$62\cdot10^{-5}$	1.29
	4	12453	2713	$3229\cdot10^{-5}$	15.74	8761	1404	$93\cdot10^{-5}$	2.75
GM GQN	1	–	–	–	–	21	500	$1\cdot10^{-5}$	0.67
	2	–	–	–	–	221	586	$5\cdot10^{-5}$	0.48
	3	–	–	–	–	1581	807	$15\cdot10^{-5}$	0.38
	4	–	–	–	–	8761	1461	$15\cdot10^{-5}$	0.37
PA	1	23	467	$4\cdot10^{-5}$	0.14	21	328	$7\cdot10^{-5}$	0.03
	2	243	583	$7\cdot10^{-5}$	$2\cdot10^{-3}$	201	382	$8\cdot10^{-5}$	$2\cdot10^{-4}$
	3	1607	916	$7\cdot10^{-5}$	$4\cdot10^{-5}$	1201	713	$8\cdot10^{-5}$	$3\cdot10^{-6}$
	4	7767	5604	$7\cdot10^{-5}$	$6\cdot10^{-5}$	5281	1420	$8\cdot10^{-5}$	$6\cdot10^{-6}$

Table 3. Time requirements, probability of failure and errors in predicting safety margin for the *prescribed histograms* with model parameters $\boldsymbol{m}$.

gate for safety margin M. One can see that the estimations of failure probability are unsatisfactory for all methods examined. Predictions of the safety margin seems better in both variants, but *Variant A* significantly outperforms *Variant B*, see Figure 4. The number of random variables involved in the PCEs constructed appears to be a crucial factor here. The total number of random variables for *Variant B* is eleven, including the uncertain yield stress f_y, missing from *Variant A* PCEs except during the sampling of failure probability. Therefore, even though *Variant B* requires the construction of only one PCE, the additional variable causes an enormous increase in complexity because of an increasing polynomial degree, which also quickly increases computational times.

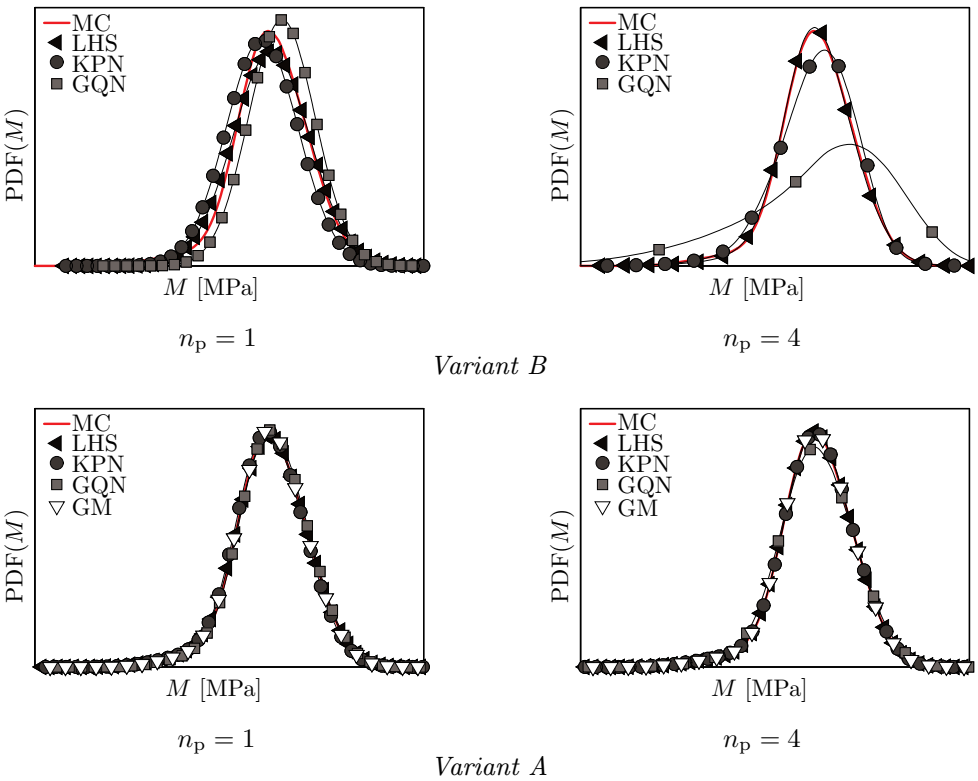

Figure 4. Probability density functions of safety margin M for different n_p for the *prescribed histograms* with model parameters $\boldsymbol{m}$.

The overall unsatisfactory results of PCE approximations are a result of a highly nonlinear transformation (equation (3.4)). This hypothesis is supported by the good results of PA. The most problematic relations are likely the transformations of parameters with the prescribed histograms $S_{\sigma 1}$, $S_{\sigma 2}$ and $L_{\sigma 1}$, $L_{\sigma 2}$, respectively, to standard normal variables, as shown in Figure 5. In order to test this assumption,

we have replaced these two prescribed histograms by new ones closer to the normal distribution, see Figure 6. The new histograms respect the initial values of means and standard deviations from the prescribed histograms.

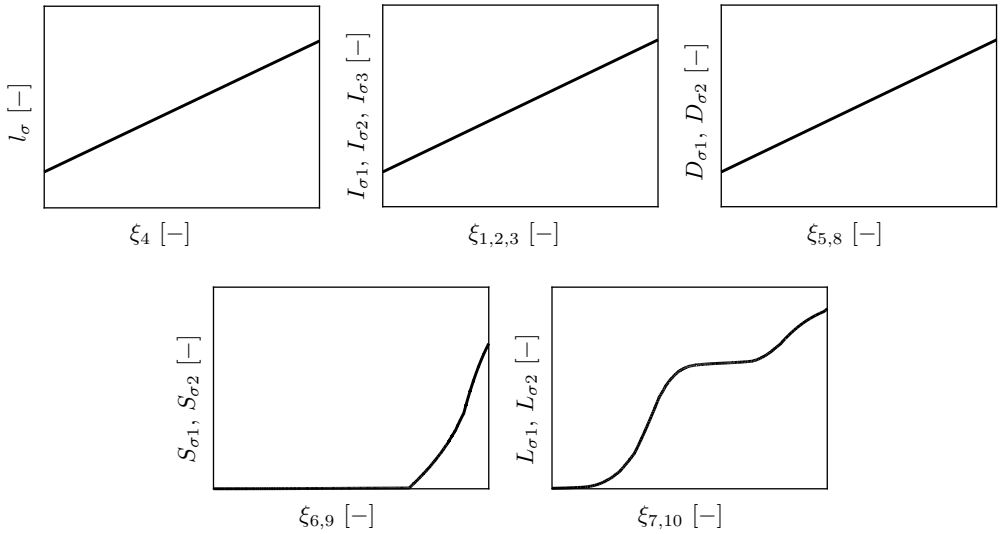

Figure 5. Transformation relations for prescribed histograms.

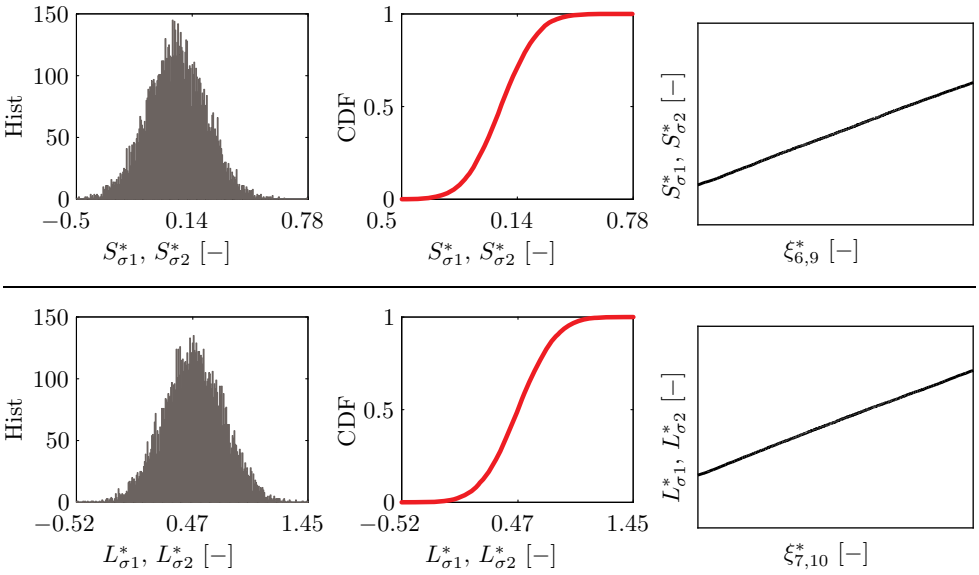

Figure 6. New histograms of model parameters with the corresponding cumulative density functions and transformation relations.

Method	n_p	n_d	Time [s]	μ_{u_A} [mm]	σ_{u_A} [mm]	μ_{w_A} [mm]	σ_{w_A} [mm]	μ_{φ_A} [mrad]	$\sigma_{\varphi_\mathrm{A}}$ [mrad]
MC	–	10^7	21874	0.206	0.033	0.009	0.002	4.056	0.789
				$\varepsilon_{\mu_{u_\mathrm{A}}}$ [%]	$\varepsilon_{\sigma_{u_\mathrm{A}}}$ [%]	$\varepsilon_{\mu_{w_\mathrm{A}}}$ [%]	$\varepsilon_{\sigma_{w_\mathrm{A}}}$ [%]	$\varepsilon_{\mu_{\varphi_\mathrm{A}}}$ [%]	$\varepsilon_{\sigma_{\varphi_\mathrm{A}}}$ [%]
LHS	1	21	0	0.01	0.91	0.13	3.06	0.02	0.02
	2	201	0	0.01	0.08	0.02	0.16	0.01	0.09
	3	1201	3	0.00	0.13	0.03	0.34	0.00	0.13
	4	5301	19	0.01	0.00	0.01	0.06	0.01	0.00
KPN	1	21	0	0.05	0.13	0.04	0.06	0.05	0.11
	2	201	0	0.05	0.09	0.04	0.00	0.05	0.09
	3	1201	3	0.01	0.27	0.01	0.19	0.01	0.26
	4	5301	13	0.01	0.13	0.01	0.13	0.01	0.13
GQN	1	21	0	0.08	0.21	0.06	0.20	0.08	0.20
	2	221	0	0.05	0.07	0.04	0.01	0.05	0.07
	3	1581	4	0.03	0.47	0.03	0.30	0.03	0.47
	4	8761	21	0.01	0.20	0.01	0.21	0.01	0.20
GM GQN	1	21	1	0.07	0.31	0.01	0.09	0.01	0.32
	2	221	0	0.07	0.35	0.01	0.15	0.01	0.28
	3	1581	3	0.07	0.35	0.01	0.16	0.01	0.21
	4	8761	41	0.07	0.36	0.01	0.17	0.01	0.07

Table 4. Time requirements and errors in predicting means and standard deviations for displacement vector components for the *new histograms* with model parameters $\boldsymbol{m}$.

Results obtained for the case of the new histograms and *Variant A* are listed in Table 4. One can see that the replacement of the two histograms led to a significant improvement in results achieved for all methods. GQN based collocation yields the worst results and the method still suffers from problems with convergence. The regression method LHS provides the worst estimation for polynomials of the first degree, but the error here decreases with increasing polynomial degree. The behaviour of the semi-intrusive Galerkin method and stochastic collocation is very similar due to numerical integration based on GQN rules.

The same improvement can be seen also in the prediction of the whole probability density function for safety margin M. The corresponding errors in predicting the safety margin and the failure probability are listed in Table 5.

We can also notice that GQN-based collocation provides the worst results for the response corresponding to the safety margin. The semi-intrusive Galerkin method delivers the worst prediction. The resulting estimation of failure probability is now satisfactory; in *Variant A*, it is excellent.

			Variant B				*Variant A*		
Method	n_{p}	n_{d}	Time [s]	$\Pr(F)$ [−]	ε_M [%]	n_{d}	Time [s]	$\Pr(F)$ [−]	ε_M [%]
MC	–	10^7	23833	$5\cdot10^{-7}$	–	10^7	21874	$5\cdot10^{-7}$	–
LHS	1	23	32	$9\cdot10^{-7}$	$2.86\cdot10^{-1}$	21	479	$5\cdot10^{-7}$	$3.20\cdot10^{-2}$
	2	243	165	$6\cdot10^{-7}$	$7.98\cdot10^{-2}$	201	537	$5\cdot10^{-7}$	$1.42\cdot10^{-2}$
	3	1607	753	$3\cdot10^{-7}$	$8.26\cdot10^{-2}$	1201	782	$5\cdot10^{-7}$	$1.43\cdot10^{-2}$
	4	7767	2701	$15\cdot10^{-7}$	$2.00\cdot10^{-1}$	5281	1437	$5\cdot10^{-7}$	$2.75\cdot10^{-2}$
KPN	1	23	31	$10\cdot10^{-7}$	$2.59\cdot10^{-1}$	21	475	$5\cdot10^{-7}$	$2.02\cdot10^{-2}$
	2	243	164	$6\cdot10^{-7}$	$8.21\cdot10^{-2}$	201	551	$5\cdot10^{-7}$	$1.32\cdot10^{-2}$
	3	1607	758	$1\cdot10^{-7}$	$1.66\cdot10^{-1}$	1201	778	$5\cdot10^{-7}$	$2.41\cdot10^{-2}$
	4	7767	2786	$8\cdot10^{-7}$	$1.30\cdot10^{-1}$	5281	1425	$5\cdot10^{-7}$	$2.20\cdot10^{-2}$
GQN	1	23	31	$10\cdot10^{-7}$	$2.41\cdot10^{-1}$	21	484	$5\cdot10^{-7}$	$2.12\cdot10^{-2}$
	2	265	164	$6\cdot10^{-7}$	$1.47\cdot10^{-1}$	221	560	$5\cdot10^{-7}$	$2.35\cdot10^{-2}$
	3	2069	763	$1\cdot10^{-7}$	$1.98\cdot10^{-1}$	1581	781	$5\cdot10^{-7}$	$3.39\cdot10^{-2}$
	4	12453	2714	$2\cdot10^{-7}$	$2.94\cdot10^{-1}$	8761	1418	$5\cdot10^{-7}$	$3.48\cdot10^{-2}$
GM GQN	1	–	–	–	–	21	491	$5\cdot10^{-7}$	$1.99\cdot10^{-2}$
	2	–	–	–	–	221	575	$5\cdot10^{-7}$	$2.67\cdot10^{-2}$
	3	–	–	–	–	1581	782	$5\cdot10^{-7}$	$4.03\cdot10^{-2}$
	4	–	–	–	–	8761	1446	$6\cdot10^{-7}$	$4.45\cdot10^{-2}$

Table 5. Time requirements, probability of failure and errors in predicting safety margin for the *new histograms* with model parameters $\boldsymbol{m}$.

In both previous examples, the discrete nature of prescribed histograms led to the necessity of numerical integration in the stochastic Galerkin method resulting in its semi-intrusive variant. In order to investigate the performance of the fully intrusive stochastic Galerkin method avoiding all numerical approximations, we have changed the prescribed distributions for model parameters once more. This time, we assume all the parameters to be normally distributed with the original values of means and standard deviations. In such cases, the transformation (3.4) becomes a 1st order polynomial and hence, analytical integration is available.

Figure 7 shows the functional dependence of safety margin M for considered types of probability distribution prescribed to model parameters. Figure 7(a) shows that the relation between M and the model parameters $\boldsymbol{m}$ is linear, while high nonlinearity appears in the relation to standard variables $\boldsymbol{\xi}$ for the prescribed histograms, see Figure 7(b). Replacement of the two histograms $S_{\sigma1}$, $S_{\sigma2}$ and $L_{\sigma1}$, $L_{\sigma2}$, respectively, with new ones more similar to normal distributions leads to an almost linear $M-\xi$ relation, namely in the high probability region, see Figure 7(c). Finally, prescription of the normal distribution to model parameters leads to a linear $M-\xi$ relation as shown in Figure 7(d).

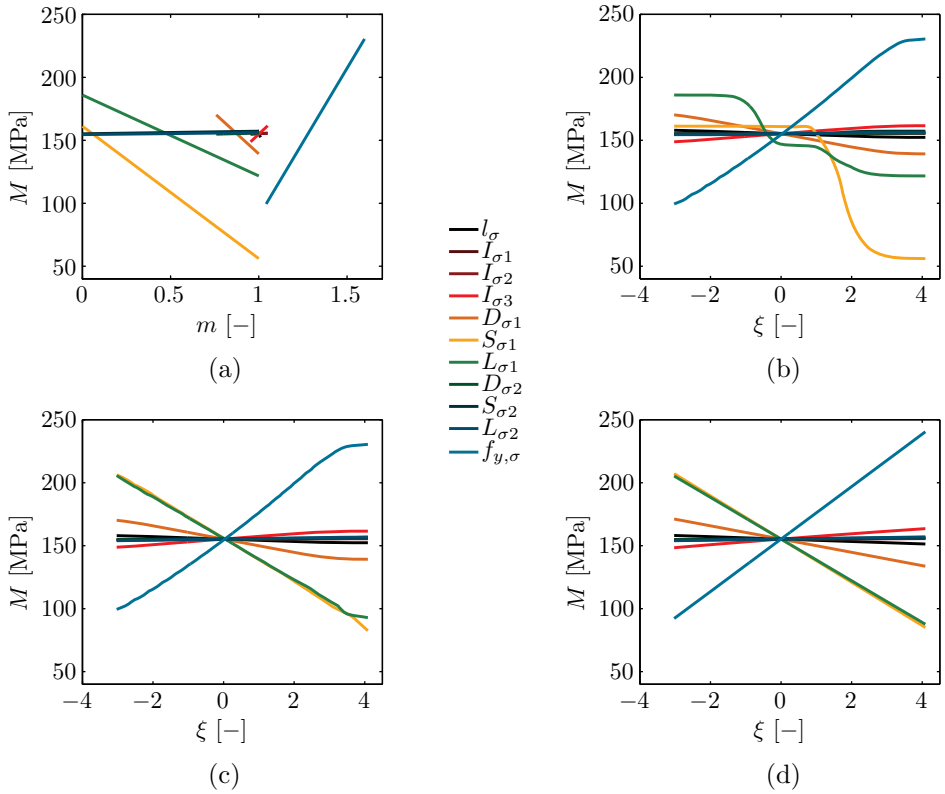

Figure 7. Functional dependence of safety margin M on model parameters $\boldsymbol{m}$ (a), on standard variables $\boldsymbol{\xi}$ for the *prescribed histograms* (b), *new histograms* (c), and *normal distribution* (d).

Results for normally distributed model parameters $\boldsymbol{m}$ and *Variant A* are shown in Table 6.

The results prove that the $u_\mathrm{A} - \xi$ relation is now linear and thus the 1st order polynomials are sufficient for constructing an excellent surrogate. The differences between the various methods here are negligible in terms of accuracy and time requirements.

Figure 8 compares the achieved accuracy in estimating the mean of displacement u_A for all variants of the presented distribution of the parameters. The graphs show convergence of the mean estimation with help of the Monte Carlo method with 10^2 to 10^7 simulations for the full numerical model compared to the estimations obtained with coefficients of polynomials of the 4th degree.

The most accurate estimation in the variant of the prescribed histograms (Figure 8(a)) is obtained with a surrogate model based on the regression method, while stochastic collocation based on GQN rules yields the worst result. For the new his-

Method	n_p	n_d	Time [s]	μ_{u_A} [mm]	σ_{u_A} [mm]	μ_{w_A} [mm]	σ_{w_A} [mm]	μ_{φ_A} [mrad]	$\sigma_{\varphi_\mathrm{A}}$ [mrad]
MC	–	10^7	3692	0.207	0.033	0.009	0.002	4.090	0.795
				$\varepsilon_{\mu_{u_\mathrm{A}}}$ [%]	$\varepsilon_{\sigma_{u_\mathrm{A}}}$ [%]	$\varepsilon_{\mu_{w_\mathrm{A}}}$ [%]	$\varepsilon_{\sigma_{w_\mathrm{A}}}$ [%]	$\varepsilon_{\mu_{\varphi_\mathrm{A}}}$ [%]	$\varepsilon_{\sigma_{\varphi_\mathrm{A}}}$ [%]
LHS	1	21	0	$5.2\cdot10^{-2}$	0.2800	$5.8\cdot10^{-2}$	0.5300	$6.6\cdot10^{-2}$	0.5800
	2	201	0	$7.9\cdot10^{-3}$	0.0140	$6.8\cdot10^{-3}$	0.0042	$7.5\cdot10^{-3}$	0.0059
	3	1201	2	$7.9\cdot10^{-3}$	0.0069	$5.5\cdot10^{-3}$	0.0032	$7.9\cdot10^{-3}$	0.0029
	4	5301	10	$7.9\cdot10^{-3}$	0.0069	$5.5\cdot10^{-3}$	0.0032	$7.9\cdot10^{-3}$	0.0029
KPN	1	21	0	$7.9\cdot10^{-3}$	0.0490	$5.5\cdot10^{-3}$	0.0530	$7.9\cdot10^{-3}$	0.0260
	2	201	0	$7.9\cdot10^{-3}$	0.0069	$5.5\cdot10^{-3}$	0.0032	$7.9\cdot10^{-3}$	0.0029
	3	1201	0	$7.9\cdot10^{-3}$	0.0069	$5.5\cdot10^{-3}$	0.0032	$7.9\cdot10^{-3}$	0.0029
	4	5301	3	$7.9\cdot10^{-3}$	0.0069	$5.5\cdot10^{-3}$	0.0032	$7.9\cdot10^{-3}$	0.0029
GQN	1	21	0	$7.9\cdot10^{-3}$	0.0050	$5.5\cdot10^{-3}$	0.0530	$7.9\cdot10^{-3}$	0.0260
	2	221	0	$7.9\cdot10^{-3}$	0.0069	$5.5\cdot10^{-3}$	0.0031	$7.9\cdot10^{-3}$	0.0029
	3	1581	1	$7.9\cdot10^{-3}$	0.0069	$5.5\cdot10^{-3}$	0.0032	$7.9\cdot10^{-3}$	0.0029
	4	8761	5	$7.9\cdot10^{-3}$	0.0069	$5.5\cdot10^{-3}$	0.0032	$7.9\cdot10^{-3}$	0.0029
GM	1	–	0	$7.9\cdot10^{-3}$	0.0045	$5.5\cdot10^{-3}$	0.0500	$7.9\cdot10^{-3}$	0.0170
	2	–	0	$7.9\cdot10^{-3}$	0.0069	$5.5\cdot10^{-3}$	0.0031	$7.9\cdot10^{-3}$	0.0029
	3	–	3	$7.9\cdot10^{-3}$	0.0069	$5.5\cdot10^{-3}$	0.0032	$7.9\cdot10^{-3}$	0.0029
	4	–	45	$7.9\cdot10^{-3}$	0.0069	$5.5\cdot10^{-3}$	0.0032	$7.9\cdot10^{-3}$	0.0029

Table 6. Time requirements and errors in predicting mean and standard deviation of displacement vector components for *normal distribution* with model parameters $\boldsymbol{m}$.

tograms (Figure 8(b)), all methods except the semi-intrusive Galerkin method provide very accurate results. The last graph in Figure 8(c) shows excellent estimations for all methods investigated.

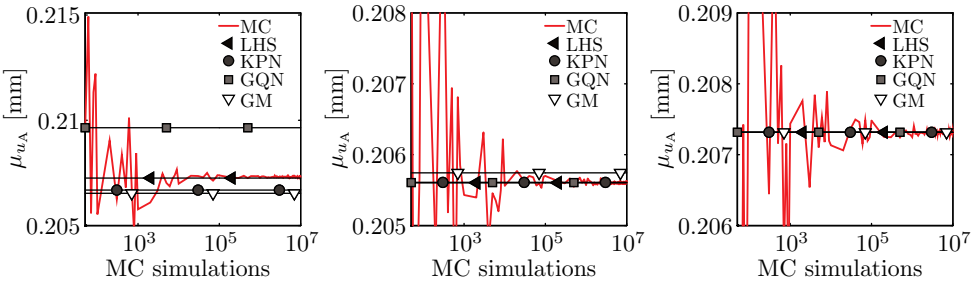

Figure 8. Comparison of the predicted mean of displacement u_A based on PCE and MC with different numbers of simulations for the *prescribed histograms* (a), *new histograms* (b), and *normal distribution* (c).

The errors in prediction of safety margin and failure probability are given in Table 7. The $M - \xi$ relation is now linear and thus the 1st order polynomials are sufficient for constructing an excellent surrogate using all the particular methods.

		Variant B				*Variant A*			
Method	n_p	n_d	Time [s]	$\Pr(F)$ [−]	ε_M [%]	n_d	Time [s]	$\Pr(F)$ [−]	ε_M [%]
MC	–	10^7	3819	$12 \cdot 10^{-7}$	–	10^7	3773	$12 \cdot 10^{-7}$	–
LHS	1	23	32	$12 \cdot 10^{-7}$	$1.14 \cdot 10^{-1}$	19	439	$12 \cdot 10^{-7}$	$2.49 \cdot 10^{-2}$
	2	243	179	$12 \cdot 10^{-7}$	$2.10 \cdot 10^{-3}$	163	515	$12 \cdot 10^{-7}$	$2.50 \cdot 10^{-4}$
	3	1607	802	$12 \cdot 10^{-7}$	$4.17 \cdot 10^{-5}$	871	738	$12 \cdot 10^{-7}$	$3.05 \cdot 10^{-6}$
	4	7789	2987	$12 \cdot 10^{-7}$	$1.35 \cdot 10^{-6}$	3481	1374	$12 \cdot 10^{-7}$	$4.88 \cdot 10^{-8}$
KPN	1	23	38	$12 \cdot 10^{-7}$	$7.42 \cdot 10^{-2}$	19	447	$12 \cdot 10^{-7}$	$1.34 \cdot 10^{-2}$
	2	243	214	$12 \cdot 10^{-7}$	$1.30 \cdot 10^{-3}$	163	521	$12 \cdot 10^{-7}$	$1.49 \cdot 10^{-4}$
	3	1607	875	$12 \cdot 10^{-7}$	$3.32 \cdot 10^{-5}$	871	725	$12 \cdot 10^{-7}$	$2.21 \cdot 10^{-6}$
	4	7789	2997	$12 \cdot 10^{-7}$	$1.00 \cdot 10^{-6}$	3481	1362	$12 \cdot 10^{-7}$	$4.08 \cdot 10^{-8}$
GQN	1	23	31	$12 \cdot 10^{-7}$	$7.42 \cdot 10^{-2}$	19	444	$12 \cdot 10^{-7}$	$1.34 \cdot 10^{-2}$
	2	265	212	$12 \cdot 10^{-7}$	$1.30 \cdot 10^{-3}$	181	520	$12 \cdot 10^{-7}$	$1.49 \cdot 10^{-4}$
	3	2069	848	$12 \cdot 10^{-7}$	$3.32 \cdot 10^{-5}$	1177	734	$12 \cdot 10^{-7}$	$2.21 \cdot 10^{-6}$
	4	12453	2796	$12 \cdot 10^{-7}$	$9.98 \cdot 10^{-6}$	5965	1376	$12 \cdot 10^{-7}$	$4.08 \cdot 10^{-8}$
GM	1	–	–	–	–	–	456	$12 \cdot 10^{-7}$	$1.34 \cdot 10^{-2}$
	2	–	–	–	–	–	551	$12 \cdot 10^{-7}$	$1.49 \cdot 10^{-4}$
	3	–	–	–	–	–	746	$12 \cdot 10^{-7}$	$2.21 \cdot 10^{-6}$
	4	–	–	–	–	–	1425	$12 \cdot 10^{-7}$	$4.07 \cdot 10^{-8}$

Table 7. Time requirements, probability of failure and errors in predicting safety margin for *normal distribution* with model parameters $\boldsymbol{m}$.

5. Conclusion

The paper presents a survey and comparison of three methods for the construction of a polynomial chaos-based surrogate for a numerical model assuming random model parameters. The methods investigated include the regression method based on Latin Hypercube Sampling, stochastic collocation, and the stochastic Galerkin method. Particular features of these methods are discussed in the paper. The quality of obtained surrogates in terms of accuracy and time requirements is demonstrated using a comparison to the traditional Monte Carlo method with a frame structure serving as a simple illustrative example.

To obtain a PCE-based surrogate model, specific orthogonal polynomials corresponding to the probability distribution of the underlying variables must be used. The orthogonality enables computing statistical moments of approximated model re-

sponse analytically so PCE can be used very efficiently in uncertainty quantification as well as in sensitivity analysis. In this study, Hermite polynomials are employed to approximate a model response as a function of standard normal variables. The regression method provides the most accurate PCE-based approximation and thus the best results for uncertainty quantification. The stochastic collocation method has a problem with convergence. The semi-intrusive stochastic Galerkin method behaves similarly to the collocation method, because the same quadrature rules are used for numerical integration in both methods. The stochastic Galerkin method is also employed in its fully intrusive form, where all numerical estimations are eliminated and integration is performed analytically. Results of this form of the stochastic Galerkin method are good, but it is worth mentioning that the application of this method is more complicated than for the other methods, because reformulation of the full numerical model is required.

In terms of time requirements, all the methods investigated are comparable and, in comparison to the Monte Carlo method, they are significantly less time-consuming. The goal of the example presented is to predict the probability of failure of a simple engineering structure. For this, two variants of PCE applications are analyzed: *A*) approximation of selected structural displacements and rotations, *B*) approximation of safety margin. It is worth mentioning that for *Variant B*, where PCE approximates the safety margin, PCE involves one additional random variable—yield stress—and the dimension of PCE is thus by one higher than for *Variant A*. On the other hand, for *Variant A*, we approximate a set of five displacements and rotations by constructing five PCEs. From Tables 2, 4 and 6 we can conclude that the time required for construction of the PCEs (including the evaluation of model simulations for LHS or stochastic collocation) is negligible and most of the computational time is needed for repeated evaluations of PCE within the sampling of failure probability. Computational time grows exponentially with the number of variables and polynomial order. We can thus point out that evaluating five ten-dimensional PCEs is faster than the evaluation of one eleven-dimensional PCE up to the second order. With the third order, the computational time needed for evaluation of one eleven-dimensional PCE becomes increasingly more demanding.

The paper also demonstrates the practical aspects of PCE application related to nonlinearity of the approximated relationship. Results in Table 7 correspond to a utopian situation, where the approximated relationship is linear (see Fig. 7d). The approximation is thus exact even in the case of the first order PCE for both variants *A* and *B*. This leads to significant time savings.

In order to benefit from the orthogonality of the polynomial basis w.r.t. the distribution of random variables, we have to involve some transformation from some

chosen standard distribution in the case of the random variables defined by histograms. The nonlinearity of the approximated relationship thus consists not only of nonlinearity of the relationship between model responses and random inputs, but also of the transformation from standard random variables. Results in Tables 4 and 5 correspond to such a situation, with random inputs defined by histograms very close to normal distribution and a nearly linear underlying transformation, see Fig. 7c. Nevertheless, the predictions of failure probability are remarkably worse for *Variant B*; for *Variant A*, they are still precise. This is because of the yield stress involved in the *Variant B* PCE. Its transformation is nonlinear only in the low probability region, but this small nonlinearity is important due to high sensitivity of the safety margin for this input (according to Fig. 7c, it belongs to the three most important inputs). We can conclude that nonlinearity, even in only low probability regions, is significant for predicting failure probability.

Finally, an even more significant difference between the two variants is demonstrated in Table 3 for the prescribed histograms taken from the literature. Fig. 2 reveals that the histograms prescribed to short- and long-lasting loads are far from exhibiting normal distributions, and the corresponding transformation from normal variables depicted in Fig. 5 is highly nonlinear. This nonlinearity is thus remarkable, also in the approximated relationship of the safety margin, as is visible in Fig. 7b. This nonlinearity is present equally in both variants, but predictions for *Variant B* worsened more significantly (even in terms of orders), although the difference in both variants did not change and consists only of an additional variable—yield stress—for *Variant B*. Therefore, significantly worse results for *Variant B* compared to *Variant A* are caused only by a slightly higher dimension for the approximated relationship.

We thus conclude that failure probability is extremely sensitive to approximation errors. This is related namely to the nonlinearity and dimensionality of the approximated relationship. The results presented show that—regarding the computational time and accuracy of predictions—it is more efficient to construct a set of five ten-dimensional approximations than one approximation with eleven dimensions. Moreover, when applying orthogonal polynomial chaos, it is important to be careful when introducing nonlinear transformations to standard random variables.

References

[1] *F. Augustin, A. Gilg, M. Paffrath, P. Rentrop, M. Villegas, U. Wever*: An accuracy comparison of polynomial chaos type methods for the propagation of uncertainties. J. Math. Ind. *3* (2013), 24 pages. zbl MR doi

[2] *I. Babuška, F. Nobile, R. Tempone*: A stochastic collocation method for elliptic partial differential equations with random input data. SIAM J. Numer. Anal. *45* (2007), 1005–1034. zbl MR doi

[3] *I. Babuška, R. Tempone, G. E. Zouraris*: Galerkin finite element approximations of stochastic elliptic partial differential equations. SIAM J. Numer. Anal. *42* (2004), 800–825. zbl MR doi

[4] *G. Blatman, B. Sudret*: An adaptive algorithm to build up sparse polynomial chaos expansions for stochastic finite element analysis. Probabilistic Engineering Mechanics *25* (2010), 183–197. doi

[5] *G. Blatman, B. Sudret*: Adaptive sparse polynomial chaos expansion based on least angle regression. J. Comput. Phys. *230* (2011), 2345–2367. zbl MR doi

[6] *H. Cheng, A. Sandu*: Efficient uncertainty quantification with the polynomial chaos method for stiff systems. Math. Comput. Simul. *79* (2009), 3278–3295. zbl MR doi

[7] *S.-K. Choi, R. V. Grandhi, R. A. Canfield, C. L. Pettit*: Polynomial chaos expansion with latin hypercube sampling for estimating response variability. AIAA J. *42* (2004), 1191–1198. doi

[8] *O. Ditlevsen, H. O. Madsen*: Structural Reliability Methods. John Wiley & Sons, Chichester, 1996.

[9] *M. Eigel, C. J. Gittelson, C. Schwab, E. Zander*: Adaptive stochastic Galerkin FEM. Comput. Methods Appl. Mech. Eng. *270* (2014), 247–269. zbl MR doi

[10] *M. S. Eldred, J. Burkardt*: Comparison of non-intrusive polynomial chaos and stochastic collocation methods for uncertainty quantification. The 47th AIAA Aerospace Sciences Meeting including The New Horizons Forum and Aerospace Exposition, Orlando. AIAA 2009-976, 2009, pp. 20. doi

[11] *H. C. Elman, C. W. Miller, E. T. Phipps, R. S. Tuminaro*: Assessment of collocation and Galerkin approaches to linear diffusion equations with random data. Int. J. Uncertain. Quantif. *1* (2011), 19–33. zbl MR doi

[12] *A. Fülöp, M. Iványi*: Safety of a column in a frame. Probabilistic Assessment of Structures Using Monte Carlo Simulation: Background, Exercises and Software (P. Marek et al., eds.). Institute of Theoretical and Applied Mechanics, Academy of Sciences of the Czech Republic, Praha, CD, Chapt. 8.10, 2003.

[13] *R. G. Ghanem, P. D. Spanos*: Stochastic Finite Elements: A Spectral Approach, Revised Edition. Dover Civil and Mechanical Engineering, Dover Publications, 2012. zbl MR doi

[14] *M. Gutiérrez, S. Krenk*: Stochastic finite element methods. Encyclopedia of Computational Mechanics (E. Stein et al., eds.). John Wiley & Sons, Chichester, 2004. zbl MR doi

[15] *F. Heiss, V. Winschel*: Likelihood approximation by numerical integration on sparse grids. J. Econom. *144* (2008), 62–80. zbl MR doi

[16] *S. Hosder, R. W. Walters, M. Balch*: Efficient sampling for non-intrusive polynomial chaos applications with multiple uncertain input variables. The 48th AIAA/ASME/ASCE/AHS/ASC Structures, Structural Dynamics and Materials Conference, Honolulu. AIAA 2007-1939, 2007, pp. 16. doi

[17] *C. Hu, B. D. Youn*: Adaptive-sparse polynomial chaos expansion for reliability analysis and design of complex engineering systems. Struct. Multidiscip. Optim. *43* (2011), 419–442. zbl MR doi

[18] *E. Janouchová, A. Kučerová*: Competitive comparison of optimal designs of experiments for sampling-based sensitivity analysis. Comput. Struct. *124* (2013), 47–60. doi

[19] *E. Janouchová, A. Kučerová, J. Sýkora*: Polynomial chaos construction for structural reliability analysis. Proceedings of the Fourth International Conference on Soft Computing Technology in Civil, Structural and Environmental Engineering (Y. Tsompanakis et al., eds.). Civil-Comp Press, Stirlingshire, 2015, Paper 9. doi

[20] *J. Li, J. Li, D. Xiu*: An efficient surrogate-based method for computing rare failure probability. J. Comput. Phys. *230* (2011), 8683–8697. zbl MR doi

[21] *J. Li, D. Xiu*: Evaluation of failure probability via surrogate models. J. Comput. Phys. *229* (2010), 8966–8980. zbl MR doi
[22] *X. Ma, N. Zabaras*: An adaptive hierarchical sparse grid collocation algorithm for the solution of stochastic differential equations. J. Comput. Phys. *228* (2009), 3084–3113. zbl MR doi
[23] *H. G. Matthies*: Uncertainty quantification with stochastic finite elements. Encyclopedia of Computational Mechanics (E. Stein et al., eds.). John Wiley & Sons, Chichester, 2007. zbl MR doi
[24] *H. G. Matthies, A. Keese*: Galerkin methods for linear and nonlinear elliptic stochastic partial differential equations. Comput. Methods Appl. Mech. Eng. *194* (2005), 1295–1331. zbl MR doi
[25] *H. N. Najm*: Uncertainty quantification and polynomial chaos techniques in computational fluid dynamics. Annual Review of Fluid Mechanics 41 (S. H. Davis et al., eds.). Annual Reviews, Palo Alto, 2009, pp. 35–52. zbl MR doi
[26] *F. Nobile, R. Tempone, C. G. Webster*: A sparse grid stochastic collocation method for partial differential equations with random input data. SIAM J. Numer. Anal. *46* (2008), 2309–2345. zbl MR doi
[27] *M. Paffrath, U. Wever*: Adapted polynomial chaos expansion for failure detection. J. Comput. Phys. *226* (2007), 263–281. zbl MR doi
[28] *M. P. Pettersson, G. Iaccarino, J. Nordström*: Polynomial chaos methods. Polynomial Chaos Methods for Hyperbolic Partial Differential Equations. Numerical Techniques for Fluid Dynamics Problems in the Presence of Uncertainties. Mathematical Engineering, Springer, Cham, 2015, pp. 23–29. zbl MR doi
[29] *R. Pulch*: Stochastic collocation and stochastic Galerkin methods for linear differential algebraic equations. J. Comput. Appl. Math. *262* (2014), 281–291. zbl MR doi
[30] *G. Stefanou*: The stochastic finite element method: Past, present and future. Comput. Methods Appl. Mech. Eng. *198* (2009), 1031–1051. zbl doi
[31] *N. Wiener*: The homogeneous chaos. Am. J. Math. *60* (1938), 897–936. zbl MR doi
[32] *D. Xiu*: Fast numerical methods for stochastic computations: A review. Commun. Comput. Phys. *5* (2009), 242–272. zbl MR
[33] *D. Xiu*: Numerical Methods for Stochastic Computations: A Spectral Method Approach. Princeton University Press, Princeton, 2010. zbl MR doi
[34] *D. Xiu, J. S. Hesthaven*: High-order collocation methods for differential equations with random inputs. SIAM J. Sci. Comput. *27* (2005), 1118–1139. zbl MR doi

Authors' address: *Eliška Janouchová*, *Jan Sýkora*, *Anna Kučerová*, Czech Technical University in Prague, Faculty of Civil Engineering, Department of Mechanics, Thákurova 7, 166 29 Praha 6, Czech Republic, e-mail: `eliska.janouchova@fsv.cvut.cz`, `jan.sykora.1@fsv.cvut.cz`, `Anna.Kucerova@cvut.cz`.